INSTITUTE OF PHYSICS PUBLISHING JOURNAL OF PHYSICS B: ATOMIC, MOLECULAR AND OPTICAL PHYSICS

J. Phys. B: At. Mol. Opt. Phys. **37** (2004) S127–S139 PII: S0953-4075(04)71247-X

Vortex nucleation through edge states in finite Bose–Einstein condensates

Eric Akkermans and Sankalpa Ghosh

Physics Department, Technion IIT, Haifa-32000, Israel

Received 30 October 2003, in final form 4 February 2004
Published 24 March 2004
Online at stacks.iop.org/JPhysB/37/S127 (DOI: 10.1088/0953-4075/37/7/059)

Abstract

We study the vortex nucleation in a finite Bose–Einstein condensate. Using a set of non-local and chiral boundary conditions to solve the Schrödinger equation of non-interacting bosons in a rotating trap, we obtain a quantitative expression for the characteristic angular velocity for vortex nucleation in a condensate which is found to be 35% of the transverse harmonic trapping frequency.

1. Introduction

A prominent feature of a superfluid is the way it behaves under rotation [1]. In contrast to a normal fluid, which rotates like a rigid body at thermal equilibrium, the thermodynamically stable state of a superfluid at low enough frequency does not rotate. At higher frequencies, a finite amount of angular momentum appears in the form of vortex filaments at which the superfluid density vanishes. The circulation of the velocity field flow evaluated on a closed contour that encircles the vortex is quantized [2, 3]. This is a consequence of the existence of a macroscopic wavefunction, whose phase changes by an integer multiple of 2π around the vortex filaments. Atomic Bose–Einstein condensates (BEC) [4, 5] provide a reference system where the superfluid behaviour can be studied in the weak-coupling regime.

A set of recent experiments have demonstrated [6–14] the existence of vortices in atomic condensates. The rotational frequency at which the first vortex is nucleated has been shown to depend on parameters such as the trap geometry (aspect ratio), the nature and the characteristic time of the stirring beam, the number of atoms in the trap and may therefore vary from one experiment to another. The ratio of this characteristic rotational frequency to the transverse harmonic trapping frequency varies in these experiments from 0.1 [12] to 0.7 [9].

Most of the theoretical studies of vortex nucleation in atomic BEC which preceded these experiments [15–20], determine the characteristic nucleation frequency of the first vortex from the criterion that the vortex state becomes the minimum of the thermodynamic free energy of the system evaluated in the co-rotating frame. In [21] the global as well as local stability of the vortex state is discussed within the framework of the Bogoliubov

 © 2004 IOP Publishing Ltd Printed in the UK

theory [3]. Using the Thomas–Fermi approximation, the thermodynamic characteristic frequency can be expressed [16, 17] in terms of the other system parameters. These works have been reviewed in [22]. The characteristic rotational frequency of the vortex nucleation thus obtained is generally lower than the values observed experimentally [7, 8, 12].

The presence of a vortex in a static condensate is associated with an extra energy relative to the vortex free state. Using the Thomas–Fermi approximation it can be shown that this energy is the highest when the vortex is located at the centre of the trap and decreases monotonically as a function of the distance between the centre of the vortex and the centre of the trap [22–24]. Within the Thomas–Fermi approximation (without any boundary correction) it can be shown that this energy vanishes at the boundary of the system. Thus we can define the energy of a vortex state E_v as a function of the distance d, namely the separation between the vortex and the centre of the trap and $E_v(d)$ has a maximum at $d = 0$. For an increasing rotational frequency this maximum is shifted from the centre to the boundary of the system [22, 23] and at rotational frequencies higher than the thermodynamic characteristic frequency this leads to a surface energy barrier to the nucleation of a vortex. This explains why a vortex cannot be nucleated in a trapped condensate even though the trap is rotated at the thermodynamic characteristic frequency. The characteristic frequency for the vortex nucleation can be determined if one knows under what condition and at what rotational frequency a state carrying finite angular momentum will be transferred from the surface to the bulk of the condensate by overcoming the surface energy barrier. Theoretical studies in this direction have been done in [23, 25–32]. They are based on an analysis of the collective excitations localized at the surface of the condensate, namely the surface modes [33]. These modes appear as shape deformations that carry a finite angular momentum about the axis of rotation [28] and have no radial node. In a rotated condensate these surface modes are excited and this leads to the vortex nucleation. A generalization of the Landau criterion [4, 28, 34] allows us to determine at what rotational frequency the surface mode corresponding to a given angular momentum quantum number is excited and leads to the nucleation of a vortex. The characteristic nucleation determined in this way agrees with the experimentally observed value [30]. Vortices are also nucleated by exciting a particular surface mode through a controlled trap deformation [9, 14] and this problem has been theoretically studied in [23, 29].

Thus far theoretical studies of the problem of vortex nucleation in a trapped condensate have been conducted in the framework of interacting bosons using various approximation schemes. It is also known that the stable state of a set of non-interacting bosons in an axisymmetric harmonic trap does not have a finite angular momentum along the z-direction for a rotational frequency less than the trap frequency. A finite amount of interaction makes vortex states energetically feasible at a lower rotational frequency. In this paper we study the nucleation of a vortex from the surface to the bulk of a system by solving the one-particle Schrödinger equation with a set of non-local and chiral boundary conditions. To that purpose we start by discussing in section 2 the role of boundary conditions in a many-body problem. In section 3, we review the problem of a trapped boson rotating at a given frequency in an infinite plane and briefly discuss the corresponding energy spectrum in a finite disc while applying Dirichlet boundary conditions. In section 4 we introduce the chiral boundary conditions for rotating bosons in a disc and show how the Hilbert space splits into bulk and edge states. We subsequently analyse the nucleation mechanism, i.e. the transfer of angular momentum from the edge to the bulk. The characteristic angular rotation is given in terms of the trap frequency at which the first and then successive vortices are nucleated in the bulk. The variation of the size of the bulk region with increasing rotation is discussed and its physical implication is pointed out.

2. Role of the boundary conditions in a many-body problem

We start with the following Hamiltonian corresponding to N interacting bosons of mass m:

$$H_{mb} = \sum_{i=1}^{N} -\frac{\hbar^2}{2m}\nabla_i^2 + \sum_{i,j} V(|\boldsymbol{r}_i - \boldsymbol{r}_j|) - E_0 \tag{1}$$

where E_0 is the ground state energy. Except for some specific cases, one does not know how to diagonalize this Hamiltonian. Therefore some approximation schemes must be defined whose purpose is to obtain an effective quadratic Hamiltonian. We may consider, for instance, the Feynman description [35] that accounts for the excited states in the form

$$\phi(\boldsymbol{r}_1, \ldots, \boldsymbol{r}_N) = F\phi_0(\boldsymbol{r}_1, \ldots, \boldsymbol{r}_N) \tag{2}$$

where ϕ_0 is the exact but an unknown ground state wavefunction such that $H_{mb}\phi_0 = 0$, and we assume that $F = \sum_i^N f(\boldsymbol{r}_i)$. Writing F as a sum over one-body terms is exact for the non-interacting problem. For the interacting case, such a decomposition assumes that the interaction is adiabatically switched on. The wavefunction $\phi(\boldsymbol{r})$ is obtained by minimizing the energy

$$E = \frac{\int \phi^* H_{mb}\phi \, \mathrm{d}^N\boldsymbol{r}}{\int |\phi|^2 \, \mathrm{d}^N\boldsymbol{r}} \tag{3}$$

where $\mathrm{d}^N\boldsymbol{r} = \mathrm{d}\boldsymbol{r}_1 \cdots \mathrm{d}\boldsymbol{r}_N$. It can be shown that [35, 36] the effective energy E can be written as

$$E = -\rho_0 \frac{\hbar^2}{2m} \int \mathrm{d}\boldsymbol{r}\, f^*(\boldsymbol{r})\nabla^2 f(\boldsymbol{r}) \tag{4}$$

where ρ_0 is the ground state density. To obtain the corresponding spectrum, we have to impose boundary conditions on $f(\boldsymbol{r})$. Assuming translational invariance, Feynman obtained that $E = \frac{\hbar^2}{2m}\left[\frac{k^2}{S(k)}\right]$, where $S(k)$ is the structure factor. In a trapped condensate the translational invariance is broken by the presence of a confinement potential. The function $f(\boldsymbol{r})$ is related to the order parameter $\Psi(\boldsymbol{r})$. The choices for boundary conditions on the order parameter $\Psi(\boldsymbol{r})$ are broad as it depends on the nature of the confining potential and on the effective one-body term generated by the interaction. It might be thus possible to take into account at least partly the effect of interactions by solving a linear Schrödinger like equation under suitable choices of boundary conditions. However in the absence of a specific relation between such boundary conditions and the effective interactions, these choices are generally guided by the nature of the problem.

In this paper, we study the vortex nucleation in a confined geometry by solving a one-particle Schrödinger equation for the condensate wavefunction $\Psi(\boldsymbol{r})$ with a set of non-local and chiral boundary conditions. Such boundary conditions have been proposed in order to deal with such nonlinear problems [37]. These boundary conditions are motivated by the following considerations. We know [23, 25–32] that the dispersion relation for the surface excitations determines the characteristic rotational frequency of vortex nucleation. The proposed boundary conditions are designed in order to provide a clear distinction between the bulk and edge states of a two-dimensional rotating boson gas. The angular momentum quantum numbers of edge states as we shall see are higher than those of bulk states. Vortices are then nucleated by transferring a state from the edge to the bulk Hilbert spaces.

3. A rotating two-dimensional boson gas

3.1. Hamiltonian and energy spectrum for the infinite plane

We consider the Hamiltonian of a trapped boson in a two-dimensional domain rotating with a uniform angular frequency Ω:

$$H = \frac{\mathbf{p}^2}{2m} + \frac{1}{2}m\omega^2 r^2 - \Omega L_z. \tag{5}$$

We define the vector potential

$$\mathbf{A}_f = \boldsymbol{f} \times \mathbf{r} \tag{6}$$

where $\boldsymbol{f} = (0, 0, f)$. The corresponding pseudo-magnetic fields may be defined by

$$\mathbf{B}_f = \boldsymbol{\nabla} \times \mathbf{A}_f = 2\boldsymbol{f} \tag{7}$$

where f is either ω or Ω so that the Hamiltonian (5) is rewritten in the two equivalent forms as

$$H = \frac{1}{2m}(\mathbf{p} - m\mathbf{A}_\omega)^2 + (\omega - \Omega)L_z \tag{8}$$

or

$$H = \frac{1}{2m}(\mathbf{p} - m\mathbf{A}_\Omega)^2 + \frac{1}{2}m(\omega^2 - \Omega^2)r^2. \tag{9}$$

For $\omega = \Omega$, this Hamiltonian is the Landau Hamiltonian of a charged particle in a transverse magnetic field written in the symmetric gauge. For this special value the centrifugal force just offsets the confinement and hence the bosonic system becomes unstable.

The eigenfunctions $\Psi_{n,l}$ and the eigenvalues $E_{n,l}$ of the Hamiltonian for the infinite plane are characterized by two integer quantum numbers n, l where $n \in \mathbb{N}, l \in \mathbb{Z}$. We define $b_\omega = m\omega/\hbar$ and $b_\Omega = m\Omega/\hbar$. The solutions of the corresponding Schrödinger equation are

$$\Psi_{n,l}(r) = C_{n,l} r^{|l|}\, \mathrm{e}^{\mathrm{i}l\theta}\, \mathrm{e}^{-\frac{b_\omega r^2}{2}}\, {}_1F_1(a, |l| + 1; b_\omega r^2) \tag{10}$$

where $a = \frac{|l| - \frac{\Omega}{\omega} l + 1}{2} - \frac{e}{4} = -n$ with $e = \frac{2E_{n,l}}{\hbar\omega}$. ${}_1F_1(a, c; x)$ is the confluent hypergeometric function [38, 39] and $C_{n,l}$ is a normalization constant. The eigenenergies are

$$E_{n,l} = \hbar\omega\left(2n + |l| - \frac{\Omega}{\omega}l + 1\right). \tag{11}$$

For $l < 0$, the eigenvalues increase with increasing Ω, whereas for $l > 0$, they decrease with increasing Ω. For $\Omega/\omega < 1$, the ground state is always characterized by $n = 0, l = 0$ so that no vortex is nucleated. For $\Omega = \omega$, the energy spectrum is made of Landau levels that are degenerate in angular momentum.

The current density in a given eigenstate is defined by

$$\mathbf{j} = \frac{\hbar}{2m\mathrm{i}}\left(\Psi^*_{n,l}\boldsymbol{\nabla}\Psi_{n,l} - \Psi_{n,l}\boldsymbol{\nabla}\Psi^*_{n,l} - 2\mathrm{i}\frac{m}{\hbar}\mathbf{A}_\Omega|\Psi_{n,l}|^2\right). \tag{12}$$

Its radial component vanishes while its azimuthal component is

$$j_\theta = \frac{\hbar}{m}\left(\frac{l}{r} - \frac{m}{\hbar}\Omega r\right)|\Psi_{n,l}|^2. \tag{13}$$

We define the angular momentum dependent radius r_l by

$$r_l = \sqrt{\frac{l}{b_\Omega}}. \tag{14}$$

For a given angular momentum state, $j_\theta(r)$ is positive for $r < r_l$ and hence it gives a paramagnetic contribution. It is negative and diamagnetic for $r > r_l$ and vanishes at $r = r_l$.

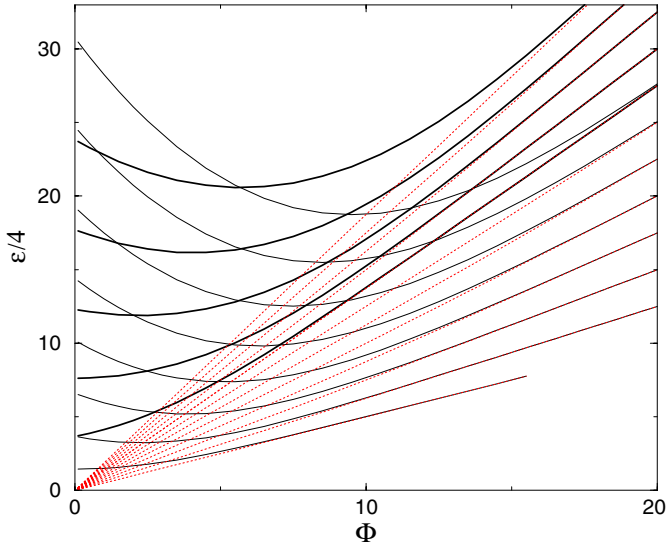

Figure 1. Energy spectrum of rotating bosons with Dirichlet boundary condition. The continuous lines (thin lines for $n = 0$ and thick lines for $n = 1$) correspond to the energy spectrum derived from (15). Each curve corresponds to a given value of the angular momentum. They correspond to $n = 0$ and $l = 0, 1, 2, 3, 4, 5, 6, 7$ as well as $n = 1$ and $l = -1, 0, 1, 2, 3$. The dotted lines represent the corresponding infinite plane solutions given by (11). Here Ω is taken to be 0.75ω.

3.2. Spectrum with Dirichlet boundary conditions (DBC)

We consider now the problem of a trapped rotating boson in a disc of radius R imposing Dirichlet boundary conditions. The corresponding spectrum is derived in the same way as for the electron in a perpendicular magnetic field [36, 40–42].

The Dirichlet boundary condition (DBC) $\Psi_{n,l}(r = R) = 0$ is according to (10) ${}_1F_1(a, |l| + 1; \Phi) = 0$ where $\Phi = b_\omega R^2$ is equivalent to the magnetic flux. The energy spectrum is obtained from the zeros of the confluent hypergeometric function ${}_1F_1$, that can be separated into two classes according to the sign of the corresponding angular momentum. For $l \geqslant 0$, the energy levels are given by

$$ {}_1F_1\left(\frac{l\left(1-\frac{\Omega}{\omega}\right)+1}{2} - \frac{\varepsilon}{4\Phi}, l+1; \Phi\right) = 0 \tag{15}$$

with $\varepsilon = \frac{2mE_{n,l}R^2}{\hbar^2} = e\Phi$. For $l < 0$ the energy levels are given by

$$ {}_1F_1\left(\frac{-l\left(1+\frac{\Omega}{\omega}\right)+1}{2} - \frac{\varepsilon}{4\Phi}, -l+1; \Phi\right) = 0. \tag{16}$$

It is important to note that the equation ${}_1F_1(a, c; x) = 0$ has solutions only for $a < 0$ and, in the interval $-p < a < -p + 1$, it has exactly p real solutions. This eliminates the possibility of having for rotating bosons, a ground state given by the lowest Landau level solution for which $\frac{\varepsilon}{4\Phi} = \frac{l(1-\frac{\Omega}{\omega})+1}{2}$.

The infinite plane solutions are reached asymptotically for large Φ (see figure 1). There is no difference in this spectrum between bulk and edge states. For $\Omega/\omega < 1$, the state $(n, l) = (0, 0)$ is always the ground state (figure 1). The energy levels become degenerate

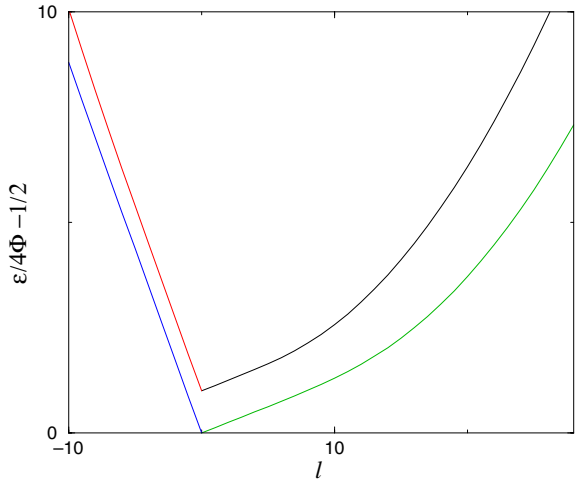

Figure 2. Edge and bulk states with DBC. The energy levels that correspond to the first two Landau levels are shown. The lower level corresponds to $n = 0$ and the upper one corresponds to $n = 1$. Φ and the ratio $\frac{\Omega}{\omega}$ are respectively taken to be 20 and 0.75.

in angular momentum when $\Omega/\omega = 1$ and $\Phi \gg 1$ [36]. Therefore at zero temperature, no vortex can be nucleated at $\Omega/\omega < 1$ under the DBC.

We have plotted the energy as a function of the angular momentum for a fixed Φ in figure 2. For the Landau problem of a charged particle in a transverse magnetic field a similar plot, but in a different geometry and only for positive angular momentum states, has been used in [43] in order to describe the role of the edge states in the quantum Hall transport. In the present problem as well as in the Landau problem there is no sharp difference between edge and bulk states under DBC.

4. Chiral boundary conditions

Dirichlet boundary conditions do not provide a way to separate edge from bulk excitations. As already pointed out, such a separation is necessary for the description of the nucleation of a vortex. We therefore propose a set of non-local and chiral boundary conditions which are more suitable for the present problem. These boundary conditions are akin to those introduced by Atiyah, Patodi and Singer (APS) in their study of index theorems for Dirac operators with boundaries [44]. Similar boundary conditions have also been applied to the Landau problem on manifolds with boundaries [41, 42]. These boundary conditions split the Hilbert space into a direct sum of two orthogonal, *infinite dimensional* spaces with positive and negative chirality on the boundary. The chirality is determined by the direction of the azimuthal velocity projected on the boundary. A vortex is nucleated as a result of the transfer of a state from the edge to the bulk.

We have already noted that for a given value of the angular momentum l, the current flows with a different chirality in regions separated by a ring of radius $r_l = \sqrt{\frac{l}{\Phi_\Omega}}$. We define the bulk and the edge regions using this particular value of r_l as a reference for a given angular momentum. The current associated with that particular angular momentum is respectively paramagnetic and diamagnetic in the bulk and the edge. Alternatively, we define the bulk

and the edge states for a disc of size R so that bulk states have angular momentum $l < b_\Omega R^2$ whereas edge states have $l \geqslant b_\Omega R^2$.

The azimuthal velocity $j_\theta(r)/|\psi(\vec{r})|^2$, projected on the boundary of the disc has eigenvalues given by

$$\lambda(R) = \frac{1}{R}(l - b_\Omega R^2) = \frac{1}{R}(l - \Phi_\Omega) \tag{17}$$

where $\Phi_\Omega = b_\Omega R^2$. The chiral boundary conditions are now defined in the following way:

For $\lambda \geqslant 0$, namely for $0 < \Phi_\Omega \leqslant l$

$$\partial_r \psi_l|_R = 0. \tag{18}$$

(For any n and henceforth we shall drop the subscript n in ψ.)

For $\lambda < 0$, namely for $l < \Phi_\Omega$

$$\left(\frac{\partial}{\partial r} + \frac{\mathrm{i}\partial}{r\partial\theta} + b_\Omega r\right)\Psi_l|_{r=R} = 0. \tag{19}$$

For the first set of wavefunctions that accounts for the edge states we use Neumann boundary conditions. We could have used as well Dirichlet boundary conditions. However, unlike Neumann boundary conditions they give an unphysical discontinuity [41]. These wavefunctions are more and more localized towards the outer side of the system for an increasing rotation frequency. For states $l < \Phi_\Omega$, which correspond to wavefunctions localized well inside the disc, we impose the mixed boundary condition (19). It is this separation in the dispersion relations of the edge states under the choice of CBC that mimics the effect of interactions. In the many-body theory of vortex nucleation this separation is achieved by solving the Bogoliubov equations under various approximations [28, 30, 32] and then by identifying the collective excitations localized at the surface of the condensate. The derivation of the spectrum under these boundary conditions is provided in detail elsewhere [45]. Here we focus on the nucleation of vortices under these boundary conditions.

Figure 3 shows the effect of an increase of the rotational frequency on the spectrum under the choice of CBC. We have plotted the energies of the bulk and the edge states for four different values of the ratio Ω/ω. For each value, the quantity Φ_Ω is increased by unit steps from 1 to 3 and the corresponding bulk and edge energies are shown. Under these conditions, the slope of the bulk energy levels increases while the slope of the edge energy levels decreases. The opposite behaviour is observed when, for a fixed Φ_Ω, the ratio Ω/ω increases. Therefore with increasing rotational frequency, states with higher angular momenta are transferred from the edge Hilbert space to the bulk Hilbert space. The lth angular momentum state is nucleated in the bulk from the edge by changing Φ_Ω from l to $l + 1$.

The plots that appear in figure 3 represent solutions of the stationary Schrödinger equation under the choice of CBC at different values of Ω and Φ_Ω. To understand the nucleation of vortices in the condensate with these solutions we use the fact that a condensate is rotated only by nucleating a vortex. Therefore in between nucleations of successive vortices, the radius of the condensate remains constant. This is in contrast to the rotation of a rigid body which flattens out continuously while increasing the rotational frequency. Let us denote by Ω_1, the characteristic frequency for nucleation of the first vortex. For a given $\Omega < \Omega_1$, the radius of the condensate is R and it corresponds to $\Phi_\Omega = 1$. The corresponding bulk and edge energy levels for $\Phi_\Omega = 1$ are obtained from (18) and (19). The condensate is therefore the bulk region that contains only the $l = 0$ state. At $\Omega = \Omega_1$, the first vortex is nucleated by transferring the $l = 1$ state from the edge to the bulk so that Φ_Ω changes from 1 to 2. Therefore, the condensate is now defined as the bulk region of $\Phi_\Omega = 2$ and it has a larger radius. The rotational flux

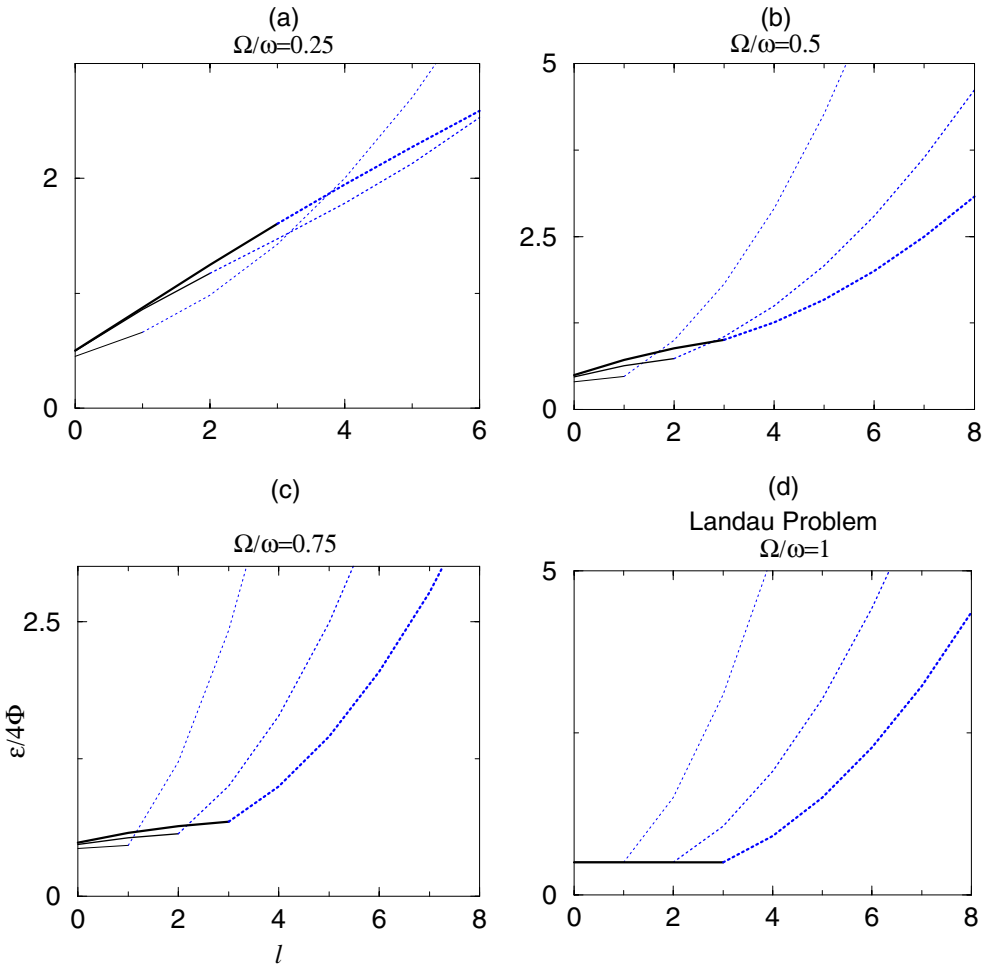

Figure 3. Effect of a faster rotation. In these figures we have plotted the energies $\varepsilon/4\Phi$ as a function of l for a set of Ω/ω values (given above each figure). The three plots in each figure correspond to $\Phi_\Omega = 1, 2, 3$ (the thinnest one for $\Phi_\Omega = 1$ and the thickest for $\Phi_\Omega = 3$). The dotted part corresponds to edge states while the continuous part corresponds to bulk states. For $\Omega/\omega = 1$ bulk states for all three values of Φ_Ω fall on the same line.

transferred by nucleating a vortex is thus h/m since this is the unit of Φ_Ω. At $\Omega = \Omega_1$, the edge states for $\Phi_\Omega = 1$ intersect the bulk states for $\Phi_\Omega = 2$. This is energetically favoured since at $\Omega = \Omega_1$, the energy $\frac{\varepsilon}{4\Phi}(l)$ of any state with $l \geqslant 2$ is less if $\Phi_\Omega = 2$ rather than $\Phi_\Omega = 1$. In the corresponding many-body description [23, 30, 32], vortices are nucleated when at a higher rotational frequency, a surface energy barrier disappears. The reduction of the edge state energy with the nucleation of a vortex is qualitatively similar to the disappearance of the surface energy barrier.

The characteristic rotational frequency for the nucleation of the first vortex determined using chiral boundary conditions (18), (19) is between $\Omega = 0.35\omega$ and 0.36ω as shown in figure 4 where ω is the transverse trap frequency. We note that this characteristic nucleation frequency is close to the value $\Omega = 0.29\omega$ that has been observed in one of the experiments on vortex nucleation [11]. All these features cannot be derived from either the infinite plane or from DBC.

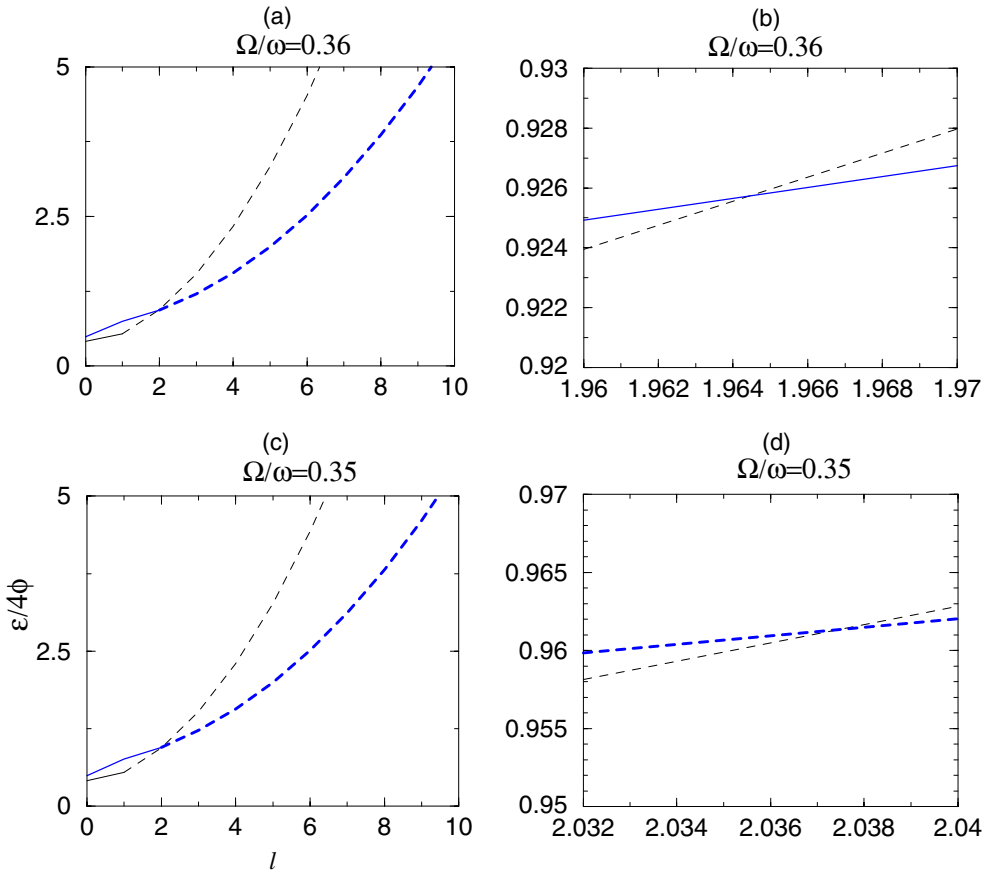

Figure 4. Determination of the characteristic frequency of vortex nucleation. In these figures we have plotted the energy $\varepsilon/4\Phi$ against the angular momentum l. The two curves in each figure correspond to $\Phi_\Omega = 1$ (thin), $\Phi_\Omega = 2$ (thick). The corresponding ratios Ω/ω are mentioned above each figure. In each curve the continuous part corresponds to bulk states and the dashed-line part to edge states. At $\Omega/\omega = 0.35$ the edge spectrum for $\Phi_\Omega = 1$ intersects the corresponding edge spectrum for $\Phi_\Omega = 2$ ((c) and (d)). At $\Omega/\omega = 0.36$, the intersection takes place between the bulk spectrum for $\Phi_\Omega = 2$ and the edge spectrum for $\Phi_\Omega = 1$ ((a) and (b)). The regions near the points of intersection are enlarged in figures (b) and (d).

To establish a parallel with the case of superconductors, let us mention similar results obtained for the vortex nucleation in a mesoscopic superconducting disc [46–48]. However, in a neutral superfluid there is no Maxwell–Ampère equation that can relate the current to the induced rotation.

5. Vortex nucleation for $\Omega > \Omega_1$

Thus far we have discussed the nucleation of the first vortex. Here we discuss the bulk and edge spectra under CBC for $\Omega > \Omega_1$. We consider the following two cases:

1. For a further increase of Ω beyond Ω_1, the edge states corresponding to $\Phi_\Omega = l$ cross the bulk states of $\Phi_\Omega = l + 1$ for $l \geqslant 2$ (figure 3). The corresponding rotational frequencies Ω_l are the nucleation frequencies of the lth vortices. Each of these vortices is nucleated by changing Φ_Ω to $\Phi_\Omega + 1$ and it carries one unit of angular momentum. Characteristic

Table 1. Nucleation frequencies of successive ($l = 1$) vortices.

Vortex	Ω/ω
1st	0.35–0.36
2nd	0.46–0.47
3rd	0.52–0.53
4th	0.569–0.57
5th	0.603–0.604
6th	0.629–0.630

Table 2. Nucleation frequencies of multiple vortices. In parentheses we mention the angular momentum states which are transferred from the edge to the bulk at these values of Ω.

No. of states transferred to the bulk	Ω/ω
2 (1, 2)	0.44–0.45
3 (1, 2, 3)	0.48–0.49
4 (1, 2, 3, 4)	0.494–0.495
5 (1, 2, 3, 4, 5)	0.498–0.499

rotational frequencies are presented in table 1. Since the bulk and edge energy spectra under CBC are obtained by solving the stationary Schrödinger equation in a co-rotating frame, solutions at different values of Ω can be related to one another if the rotation is switched on adiabatically. Such experiments [9, 14] have been performed in a deformed rotating trap where the cross-section of the rotating condensate is an ellipse in the plane of rotation. Here we solve the Schrödinger equation in a circular domain. This makes the comparison with the experimental results rather difficult. The theoretical work [29] used an approach different from ours, to explain the nucleation mechanism of the first vortex. It should also be noted that the adiabatic nucleation of successive vortices has not yet been observed experimentally. For a recent theoretical work on this issue, see [49]. One of the limitations of our theoretical framework is that we are unable to determine the spatial arrangement of more than one vortex inside the condensate.

2. Another interesting point is to find the rotational frequencies at which edge states of $\Phi_\Omega = 1$ intersect the bulk state $l = 2$ for $\Phi_\Omega = 3, 4, \ldots$. The bulk and edge energy levels of the stationary Schrödinger equations at these rotational frequencies correspond to a situation where the rotation is suddenly switched on at a frequency higher than Ω_1 and subsequently the system is brought to equilibrium in the co-rotating frame. More than one angular momentum state (and rotational flux) are transferred to the bulk at these characteristic frequencies. This leads to the nucleation of a vortex of angular momentum $l > 1$ or multiple $l = 1$ vortices at a time. Within the present theoretical framework it is not possible to identify which of these two alternatives is energetically favourable. In table 2 we have listed these rotational frequencies and the number of angular momenta transferred to the bulk Hilbert space. Around $\Omega/\omega = 0.5$, the number of vortices nucleated in this way increases very fast. Experimentally [10, 11] it has been observed that under sudden switch-on of the rotation at higher rotational frequencies more than one vortex are nucleated and the number of nucleated vortices is the largest (see, for example, figure 3 in [11]) at $\Omega = \omega/\sqrt{2}$. This is associated with a resonant quadrupolar excitation of angular momentum $l = 2$. The energy of this quadrupolar surface mode in units of the transverse trap frequency is determined within the classical hydrodynamic

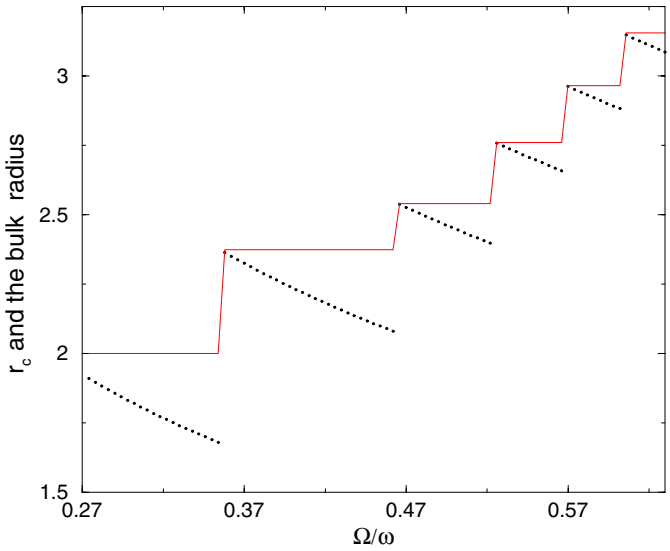

Figure 5. Size of the condensate as a function of the rotational frequency. The continuous lines give the radius of the condensate r_c as a function of Ω/ω. The dots give the radius of the bulk region for $\Phi_\Omega = l$ and for $\Omega_l < \Omega < \Omega_{l-1}$. The length is measured in units of $1/\sqrt{b_\omega}$ where $b_\omega = m\omega/\hbar$.

approximation that is very different from our approach. Therefore although our findings qualitatively agree with these experimental observations, a quantitative comparison with both the experiments and the related theory is rather involved. A reason for this is the difference in the trap geometry in the two-dimensional plane which is elliptical in the experiment while circular in our case. Another reason is the different theoretical approach that has been used to study the surface excitations in the many-body theory [27, 28, 30] and ours. The difference between the characteristic rotational frequencies in the above two cases (tables 1 and 2) thus shows that the nucleation frequency of a vortex in the condensate depends on the number of vortices already present.

The radius of the condensate is changed when a vortex is nucleated. Since a boson in the condensate has one more unit of angular momentum when a vortex is nucleated, its orbit has a larger radius. This explains why the size of the condensate region increases with successive nucleations. When the lth vortex with one unit of angular momentum is nucleated, the condensate region corresponds to $\Phi_\Omega = l + 1$. Therefore at each Ω_l, the radius of the condensate region is defined as

$$r_c|_{\Omega=\Omega_l} = \sqrt{\frac{\hbar(l+1)}{m\Omega_l}}. \tag{20}$$

Between the nucleations of the lth and $(l + 1)$th vortices, the radius of the bulk region for $\Phi_\Omega = l$ decreases as $r = \sqrt{\frac{\hbar(l+1)}{m\Omega}}$ and the corresponding edge region grows in size. In figure 5 using the set of frequencies listed in table 1 we have plotted the condensate radius. In the same figure we have simultaneously plotted the radius of the bulk region for $\Phi_\Omega = l$, in between the nucleation of the lth and $(l - 1)$th vortices. This plot involves a set of disconnected lines and the corresponding differences with the condensate region show how the edge region grows between the nucleation of two successive vortices. With the increase in the number of vortices

in the condensate these two plots get closer to one another. In the limit of a large number of vortices, the average rotation approaches the rigid body value [2, 10, 22]. For example, it has been shown in [10] that experimentally this happens when the number of vortices is around 10 [10].

Khawaja *et al* [27] have studied the surface excitations of a trapped three-dimensional Bose–Einstein condensed gas using the Gross–Pitaevskii equation and they have associated the kinetic energy of the surface region with an effective surface tension. Although our approach is different and we consider a strictly two-dimensional system, we can also define an energy associated with the edge by summing the energies of the edge states for $\Phi_\Omega = l$. For a finite system then a part of this edge energy is used to nucleate vortices.

6. Conclusion

We have presented a one-particle effective theory that describes the process of vortex nucleation in a two-dimensional rotating condensate using a set of non-local and chiral boundary conditions. We have shown that the edge states have a dispersion relation distinct from the bulk states. These boundary conditions can be understood as a way to mimic the effect of the interaction between the bosons. We have demonstrated that the properties of vortices thus nucleated agree qualitatively and quantitatively with experimental findings although a more thorough comparison is not possible in the absence of a precise mapping between this set of boundary conditions and the effective interaction. The expression of the characteristic rotational frequency at which vortices are nucleated under adiabatic and sudden switch-on of the rotation is calculated and the change in the condensate size with increasing rotation is also emphasized.

Acknowledgments

We thank the Israel Council for Higher Education for financial support. This work is supported in part by a grant from the Israel Academy of Sciences and the fund for promotion of research at the Technion.

References

[1] Legget A J 1973 *Phys. Fenn.* **8** 125
[2] Feynman R P 1955 Application of quantum mechanics to liquid helium *Progress in Low Temperature Physics I* ed C J Gorter (Amsterdam: North-Holland) chapter 2
[3] Nozieres P and Pines D 1990 *The Theory of Quantum Liquids* vol II (Reading, MA: Addison-Wesley)
[4] Pethick C and Smith H 2002 *Bose–Einstein Condensation in Dilute Gases* (Cambridge: Cambridge University Press) (for a discussion of the Landau criterion see chapter 10)
[5] Pitaevskii L and Stringari S 2003 *Bose–Einstein Condensation* (Oxford: Oxford Science Publication)
[6] Mathews M R, Anderson B P, Haljan P C, Hall D S, Weiman C E and Cornell E A 1999 *Phys. Rev. Lett.* **83** 2498
[7] Haljan P C, Coddington I, Engels P and Cornell E A 2001 *Phys. Rev. Lett.* **87** 210403
[8] Madison K W, Chevy F, Bretin V and Dalibard J 2000 *Phys. Rev. Lett.* **84** 806
Chevy F, Madison K W and Dalibard J 2000 *Phys. Rev. Lett.* **85** 2223
[9] Madison K W, Chevy F, Bretin V and Dalibard J 2001 *Phys. Rev. Lett.* **86** 4443
[10] Chevy F, Madison K W, Bretin V and Dalibard J 2001 *Preprint* cond-mat/0104218
[11] Abo Shaeer J R, Raman C, Vogels J M and Ketterle W 2001 *Science* **292** 476
[12] Raman C R, Abo-Shaeer J R, Vogels J M, Xu K and Ketterle W 2001 *Phys. Rev. Lett.* **87** 210402
[13] Rosenbusch P, Bretin V and Dalibard J 2002 *Phys. Rev. Lett.* **89** 200403
[14] Hodby E, Hechenblaikner G, Hopkins S A, Maragò O M and Foot C J 2002 *Phys. Rev. Lett.* **88** 010405

[15] Dalfovo F and Stringari S 1996 *Phys. Rev.* A **53** 2477
[16] Lundh E, Pethick C J and Smith H 1997 *Phys. Rev.* A **55** 2126
[17] Sinha S 1997 *Phys. Rev.* A **55** 4325
[18] Castin Y and Dum R 1999 *Eur. Phys. J.* D **7** 399
[19] Feder D L, Clark C W and Schneider B I 1999 *Phys. Rev. Lett.* **82** 4956
[20] Butts D A and Rokshar D S 1999 *Nature* **397** 327
[21] Isoshima T and Machida K 1999 *Phys. Rev.* A **60** 3313
[22] Fetter A L and Svidzinsky A A 2001 *J. Phys. C: Condens. Matter* **13** R135
[23] Kraemer M, Pitaevskii L, Stringari S and Zambelli F 2002 *Laser Phys.* **12** 113
[24] Guilleumas M and Graham R 2001 *Phys. Rev.* A **64** 033607
[25] Stringari S 1996 *Phys. Rev. Lett.* **77** 2360
[26] Recati A, Zambelli F and Stringari S 2001 *Phys. Rev. Lett.* **86** 377
[27] Khawaja U A, Pethick C J and Smith H 1999 *Phys. Rev.* A **60** 1507
[28] Dalfovo F and Stringari S 2000 *Phys. Rev.* A **63** 011601(R)
[29] Sinha S and Castin Y 2001 *Phys. Rev. Lett.* **87** 190402
[30] Anglin J R 2001 *Phys. Rev. Lett.* **87** 240401
Anglin J R 2002 *Phys. Rev.* A **65** 063611
[31] Muryshev A E and Fedichev P O 2001 *Preprint* cond-mat/0106462
[32] Simula T P, Virtanen S M M and Saloma M M 2002 *Phys. Rev.* A **66** 035601
[33] Onofrio R, Durfee D S, Raman C, Köhl M, Kuklewicz C E and Ketterle W 2000 *Phys. Rev. Lett.* **84** 810
[34] Landau L D 1941 *J. Phys. (USSR)* **5** 71
[35] Feynman R P 1954 *Phys. Rev.* **94** 262
[36] Akkermans E and Narevich R 1998 *Phil. Mag.* B **77** 1097
[37] Akkermans E and Mallick K 1999 *Topological Aspects of Low Dimensional Systems (Les Houches Summer School, Session LXIX)* (Berlin: Springer) (*Preprint* cond-mat/9907441) (section 3.5 is particularly relevant for the present discussion)
[38] Tricomi F G 1960 *Fonctions Hypergéometriques Confluentes (Mémorial des Sciences Mathématiques CXL)* (Paris: Gauthier-Villars)
[39] Abramowitz M and Stegun I A 1968 *Handbook of Mathematical Functions* (New York: Dover)
[40] Akkermans E, Avron J E, Narevich R and Seiler R 1998 *Eur. Phys. J.* B **1** 117–21
[41] Akkermans E and Narevich R (unpublished)
[42] Narevich R *PhD Thesis* Technion IIT, Israel (unpublished)
[43] Halperin B I 1982 *Phys. Rev.* B **25** 2185
[44] Atiyah M, Patodi V and Singer I 1975 *Math. Proc. Camb. Phys. Soc.* **77** 43
[45] Akkermans E and Ghosh S 2003 *Preprint* cond-mat/0310715
[46] Geim A K *et al* 1997 *Nature* **390** 259
Singh P, Deo S, Schweigert V A, Peeters F M and Geim A K 1997 *Phys. Rev. Lett.* **79** 4653
[47] Akkermans E and Mallick K 1999 *J. Phys. A: Math. Gen.* **32** 7133
Akkermans E, Gangardt D M and Mallik K 2000 *Phys. Rev.* B **62** 12427
[48] Bolech C, Buscaglia G C and López A 1995 *Phys. Rev.* B **52** R15179
[49] Lobo C, Sinatra A and Castin Y 2004 *Phys. Rev. Lett* **92** 020403